Journal of Chromatography A, 1599 (2019) 95–107

Contents lists available at ScienceDirect

Journal of Chromatography A

journal homepage: www.elsevier.com/locate/chroma

Evaluating the applicability of a two-dimensional liquid chromatography system for a pesticide multi-screening method

S. Muehlwald [a,*], S. Rohn [b], N. Buchner [a]

[a] Federal Office of Consumer Protection and Food Safety, Mauerstraße 39-42, 10117 Berlin, Germany
[b] University of Hamburg, Hamburg School of Food Science, Institute of Food Chemistry, Grindelallee 117, 20146 Hamburg, Germany

ARTICLE INFO

Article history:
Received 8 February 2019
Received in revised form 29 March 2019
Accepted 2 April 2019
Available online 3 April 2019

Keywords:
2D-LC
HILIC
Multi-screening
Pesticides

ABSTRACT

In this study, a fully automated two-dimensional liquid chromatography system was evaluated for pesticide analysis. The first dimension was a hydrophilic interaction liquid chromatography column for matrix separation. The analytes were collected on a trap column and transferred to the second dimension with a reversed phase column. This separation system was coupled to a quadrupole time-of-flight mass spectrometer. Investigations were started to elucidate, whether this system is useful for screening purposes. Therefore, analytes with different masses, pK_a and log K_{ow} values were chosen. The aim was to test, if broadening the scope of this method, without a time-intensive adjustment of the valve switching times is possible. All in all, the limits of the system were determined. It is important that the analytes elute from the hydrophilic interaction liquid chromatography column within a small window. It could be deduced that the window within which the analytes elute expanded too far with the chosen analytes. Therefore, optimization with different buffers, columns, column temperatures, and flow rates was started to minimise the window. Furthermore, differences in the analytes' elution behavior during hydrophilic interaction liquid chromatography separation were elucidated.

© 2019 Elsevier B.V. All rights reserved.

1. Introduction

Plant protection products contain at least one active substance. Despite proper use of plant protection products, residues of active substances (pesticide residues) and their degradation products can remain on harvested crops and in the environment [1,2]. These remaining pesticide residues in food, feed, and environment can pose a risk to human and animal health [1]. The challenges for the analysis of pesticide residues are the huge number of possible residues, the chemical diversity of the pesticides, the variety of matrices, and the control of the statutory maximum residue levels that are partly very low (<0.01 mg/kg).

The well-known *Quick Easy Cheap Effective Rugged and Safe* approach (QuEChERS) [3,4] is a common procedure for sample preparation in the analysis of pesticide residues. After homogenisation of the samples, the pesticide residues are extracted with acetonitrile. A liquid-liquid partitioning step follows to separate the pesticides from the co-extracted matrix components [3,4]. Depending on the type of sample one of various options for clean-up follows (e.g., by dispersive solid phase extraction or freezing-out) [3,4].

Two-dimensional liquid chromatography (2D-LC) is an alternative approach for the separation of complex samples. This technique has already been applied in the analysis of peptides, carbohydrates, antioxidants, and triacylglycerols [5–10]. The best results in 2D-LC separation can be achieved, when two complementary separation systems with different retention mechanism are used. This ensures a large difference between the selectivity of the separation and the retention of the sample components [5,6]. The highest degree of orthogonality in the retention mechanism can be achieved by combining hydrophilic interaction liquid chromatography (HILIC) and reverse phase chromatography (RP) [7]. Kittlaus et al. [11] had the idea to replace the traditional liquid-liquid partitioning step in QuEChERS with a HILIC column. They developed a fully automated 2D-LC system for the separation. Switching valves were used as bridging modules between the HILIC column and the RP column [7,11]. The pesticides eluted within one small window at the beginning of the 2D-LC analysis from the HILIC column. Kittlaus et al. [11] used a packed loop interface to change the solvent before the analytes were transferred to the second dimension. For this purpose, a short column was used. This allows to transfer the HILIC effluent to the RP column and to enrich all analytes in one fraction. Kittlaus et al. developed a system, coupled to a triple quadrupole mass spectrometer for the determination of over 300 pesticides [11].

* Corresponding author.
E-mail address: sandra.muehlwald@bvl.bund.de (S. Muehlwald).

https://doi.org/10.1016/j.chroma.2019.04.003
0021-9673/© 2019 Elsevier B.V. All rights reserved.

In a previous paper, we discussed the problems that could occur during the validation of a qualitative multi-screening method using QuEChERS and high-performance liquid chromatography (HPLC) with quadrupole-time-of-flight mass spectrometer (Q-TOF-MS). More than half of the analytes did not fulfil the validation criteria. Therefore, we started to elucidate reasons for the low detectability and could demonstrate that the co-eluting matrix (matrix effect) was one main cause of the signal suppression [12].

The aim of this study was to increase the detectability of the analytes that did not meet the validation criteria. Therefore, the clean-up procedure by using 2D-LC should be improved. The studies were carried out with a fully automated 2D-LC system coupled to a Q-TOF-MS.

It was aimed at evaluating, whether this system is applicable as a multi-screening method or needs to be optimized. Furthermore, it should be evaluated, whether it is possible to broaden the scope of the method developed by Kittlaus et al. [11]. Consequently, the limits of the system, with implementing as many chemically different analytes as possible, were determined.

2. Experimental

2.1. Reagents and materials

Acetonitrile (ACN), methanol (MeOH), formic acid, and acetic acid were purchased from Biosolve BV (Valkenswaard, The Netherlands). Ammonium formate and ammonium acetate were obtained from Sigma-Aldrich Production GmbH, subsidiary of Merck KGaA (Darmstadt, Germany). MiliQ water from a conventionally water treatment system was used. The pesticide standards were purchased from Sigma-Aldrich Production GmbH, subsidiary of Merck KGaA (Darmstadt, Germany), Honeywell Specialty Chemicals Seelze GmbH (Seelze, Germany), Witega GmbH (Berlin, Germany), HPC Standards GmbH (Cunnersdorf, Germany), LGC Standards GmbH (Wesel, Germany), Toronto Research Chemicals Inc. (North York, Canada) and Chem Service Inc. (West Chester, USA). The analytical standards of selected matrix components were obtained from Sigma-Aldrich Production GmbH, subsidiary of Merck KGaA (Darmstadt, Germany), Carl Roth GmbH + Co. KG (Karlsruhe, Germany), Alfa Aesar, Thermo Fisher Scientific (Karlsruhe, Germany), and Larodan AB (Solna, Sweden).

Standard solutions were prepared in diverse solvents, depending on solubility and stability. For some standard solution preparations, MeOH and ACN purchased from Biosolve BV (Valkenswaard, The Netherlands) were used. In other cases, the solutions were prepared in cyclohexane, dichloromethane, trichloromethane, ethanol, isooctane, toluene, 5 M sodium hydroxide solution, ethyl acetate, dimethyl sulfoxide, and dimethylformamide purchased from VWR GmbH (Darmstadt, Germany). The concentration of the standard solutions for the 2D-LC measurements was 100 ng/mL in ACN. Sodium hydroxide was purchased by Merck KGaA (Darmstadt, Germany).

For sample preparation the following tubes were used: Supel™ QuECitrate (EN) tube (4 g of $MgSO_4$, 1 g of NaCl, 0.5 g of $C_6H_6Na_2O_7 \times 1.5$ g of H_2O, 1 g of $C_6H_5Na_3O_7 \times 2$ g of H_2O). It was obtained from Sigma-Aldrich Production GmbH, subsidiary of Merck KGaA (Darmstadt, Germany).

2.2. Instrument and software

The 2D-LC analyses were performed with the help of the Easy Pesticides Isolation and Concentration System (EPICS) (Joint Analytical Systems GmbH (JAS), Moers, Germany). It consists of two binary pumps (Agilent Series 1100/1200, Agilent Technologies, Waldbronn, Germany), an autosampler (Agilent Series 1200, Agilent Technologies, Waldbronn, Germany), and a two-column oven (JAS, Moers, Germany). However, the heart of this system is composed of a 10-port valve (valve 1) and a 6-port valve (valve 2). Additionally, an RP pre-column was integrated into the column oven for these investigations.

2.2.1. EPICS operating principle (switching states)

The EPICS requires two binary pumps, one for the first dimension (HILIC pump) and one for the second dimension (RP pump). The HILIC column and RP column are coupled by two valves and a C8-trap column (Agilent ZORBAX-C8; 4.6 mm × 12.5 mm; 5 μm; 80 A). The valves can switch between position A and position B. Fig. 1 shows the four states and valve positions of the EPICS.

In state I, both valves are in position B (Fig. 1, state I), and the columns are conditioned. Before the first analyte (the most non-polar analyte) elutes from the HILIC column, valve 1 and valve 2 switch to position A, guiding the flow to the trap column. Additionally, the RP pump adds water to the HILIC effluent with a high flow of 2 mL/min in order to ensure the trapping of the non-polar analytes (Fig. 1, state II).

After the last analyte which could be trapped has eluted from the HILIC column, valve 2 switches back to position B. All analytes that are too polar for trapping elute from the HILIC column to the mass spectrometer, directly. Simultaneously, the flow of the RP pump stops so that the trapped pesticides remain on the trap column (Fig. 1, state III).

After elution of the last analyte (the most polar analyte) from the HILIC column, valve 1 switches to position B. The matrix components remaining on the HILIC column are flushed to the waste by applying a gradient. Simultaneously, the RP pump backflushes the trapped analytes to the RP column, where the analytes are separated by gradient elution and subsequently being transferred to the mass spectrometer (Fig. 1, state IV (valve positions are the same as for state I)). Table 1 shows an overview of the states, valve positions and default as well as adjusted valve switching times (VST).

2.2.2. Optimization of the HILIC separation

2.2.2.1. HILIC columns, gradients and eluents. The chromatographic separation in the first dimension was carried out with three HILIC columns: Column A: YMC-Pack Diol-HILIC (100 mm x 2.1 mm; 5 μm; 120 Å; YMC, Kyoto, Japan), Column B: AppliChrom OUT DiO (100 mm x 2.0 mm; 5 μm; 105 Å; AppliChrom, Oranienburg, Germany) and Column C: YMC-Triart Diol-HILIC (100 mm x 2.0 mm; 5 μm; 120 Å; YMC, Kyoto, Japan). For the HILIC separation several mobile phases were tested. Phase combination 1: Mobile phase A consisted of water and mobile phase B of ACN/water (90/10), both with 5 mM ammonium formate and 0.1% of formic acid (as recommended by JAS [13]). Phase combination 2: Mobile phase A consisted of water/buffer (95/5) and mobile phase B of ACN/water/buffer (90/5/5). The buffer consisted of 100 mM ammonium formate, pH = 3.2 (AF), and 100 mM ammonium acetate, pH = 5.8 (AA), respectively.

The gradient started with an isocratic phase of 100% of B up to 2.5 min, followed by a linear decrease to 50% of solvent B up to 7.5 min, which was maintained for 10 min. From 17.5 min to 20 min, the amount of B was increased to 100%, which was maintained for 10 and 18 min, respectively.

All investigations for the optimization of the HILIC method were carried out in a threefold determination.

2.2.2.2. Column oven temperature, buffer concentration, flow rate and injection volume. In order to decrease the window within which the analytes elute, column oven temperatures between 30 °C and 60 °C, a buffer concentration of 5 mM and 10 mM and flow rates of

Table 1
The four states of the EPICS with the default and adjusted valve switching times and valve positions for both ESI modes.

State	Default switching time [min]	Valve 1	Valve 2	Adjusted switching time in positive ESI mode [min]	Adjusted switching time in negative ESI mode [min]
I	0.0	Position B	Position B	0.0	0.0
II	1.2	Position A		0.7	0.5
II	1.3		Position A	0.8	0.6
III	2.2		Position B	1.5	1.5
IV	4.0	Position B		4.5	3.5

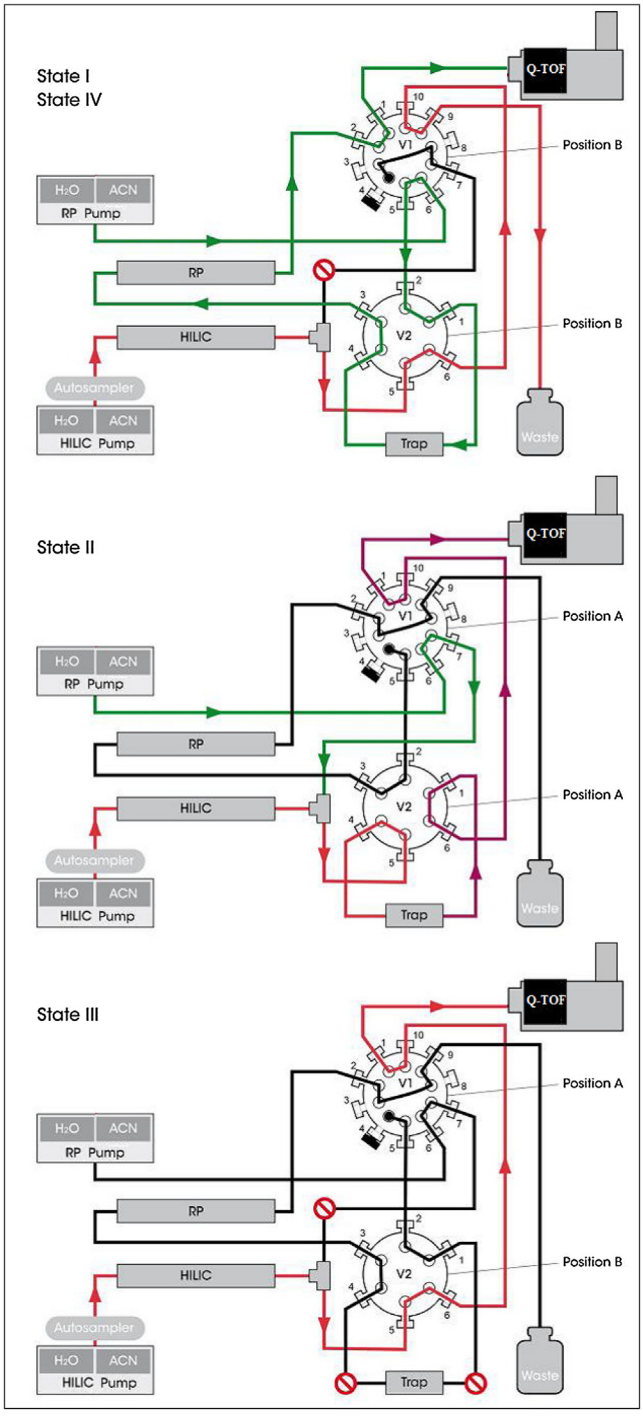

Fig. 1. Operating principle of the EPICS with the four states and the relevant valve positions. Reprinted with permission of JAS [13] and edited by us.

0.2 mL/min and 0.3 mL/min were applied. To optimize the separation by HILIC, injection volumes between 8 and 30 μL were tested.

2.2.2.3. Investigations with selected matrix components. Studies with 18 solutions of matrix components that were representative of the chosen matrix groups were carried out. These matrix components were chosen according to their log K_{ow} and pK_a values in order to cover a broad elution range. For example, these components were: chlorophyll A/B, β-carotene, histamine, nicotinic acid, bergapten, and hesperidin. It was aimed at evaluating, whether the matrix components were influenced in the same way as the analytes. Furthermore, the influence of the VST on the matrix components should be verified to evaluate the matrix separation by 2D-LC.

2.2.3. Optimization of the RP separation

2.2.3.1. RP columns, gradients and eluents. For the second dimension separation, following columns were used: RP column A: Synergi™ Fusion (150 mm x 3 mm; 4 μm; 80 Å; Phenomenex, Aschaffenburg, Germany), RP column B: ZORBAX Eclipse Plus C18 (150 mm x 2.1 mm; 3.5 μm; 95 Å; Agilent Technologies, Santa Clara, USA), RP column C: Gemini (150 mm x 2.0 mm; 5 μm; 110 Å; Phenomenex, Aschaffenburg, Germany) and RP column D: Poroshell 120 Bonus-RP (150 mm x 2.1 mm; 2.7 μm; 120 Å, Agilent Technologies, Santa Clara, USA). Moreover, a Security-Guard Cartridge Fusion RP (4 × 3.00 mm) (Phenomenex, Aschaffenburg, Germany) was used.

For the RP separation, mobile phase A consisted of water/buffer (95/5) and mobile phase B of ACN/buffer (95/5). The buffer consisted of 100 mM ammonium formate, pH = 3.2 (AF), and 100 mM ammonium acetate, pH = 5.8 (AA), respectively. Seven different gradients were tested, but the gradient development is shown by the following three examples in Fig. 2: Gradient A: oriented towards the gradient of JAS [13], Gradient B: oriented towards the gradient of our existing multi-screening method [12], and Gradient C: newly developed.

2.2.4. MS parameters

The 2D-LC system was coupled to a 6520 Q-TOF-MS (Agilent Technologies, Santa Clara, USA). The Q-TOF-MS was operated with a dual electrospray ionization (ESI) source in positive and negative ionization mode. For data acquisition, the Agilent MassHunter Workstation Software – LC/MS Data Acquisition B.06.01 was used. The following parameters were applied: gas temperature: 350 °C, drying gas: 10 L/min, fragmentor voltage: 160 V, capillary voltage: 4000 V, nebulizer pressure: 40 psig, skimmer voltage: 65 V and octapole RF: 750 V. MS spectra were recorded in the range of m/z 50–1000, with a scan rate of 5 spectra/sec and an MS absolute threshold of 200 cps.

The Agilent MassHunter Workstation Software – Qualitative Analysis B.07.00 was used for data evaluation.

Gradient A			Gradient B			Gradient C			Flow [mL/min]
Time [min]	A [%]	B [%]	Time [min]	A [%]	B [%]	Time [min]	A [%]	B [%]	
0.0	95	5	0.0	85	15	0.0	95	5	0.3
0.7	95	5	0.7	85	15	0.7	95	5	0.3
0.8	100	0	0.8	100	0	0.8	100	0	2.0
1.5	100	0	1.5	100	0	1.5	100	0	0.0
4.5	95	5	4.5	85	15	4.5	95	5	0.3
5.0	50	50	24.5	0	100	7.0	65	35	0.3
20.5	0	100	26.5	0	100	15.0	30	70	0.3
25.5	0	100	27.5	85	15	17.0	30	70	0.3
26.5	95	5	38.0	85	15	21.0	0	100	0.3
30.0	95	5				26.0	0	100	0.3
						28.0	95	5	0.3
						38.0	95	5	0.3

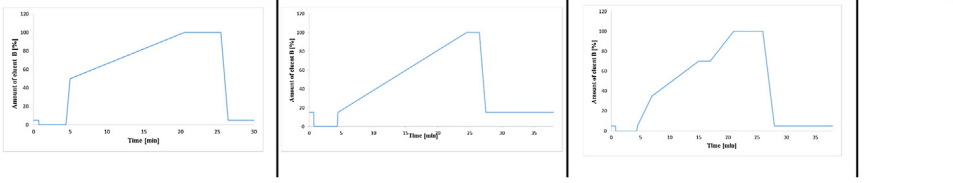

Fig. 2. Comparison of the three RP gradients for measurements in positive ESI mode. Gradient A is oriented towards the gradient of JAS [13], gradient B is oriented towards the gradient of our existing multi-screening method [12], and gradient C was newly developed.

2.3. Matrices and sample preparation

The analysed commodities were cucumber, beetroot, broccoli, leek (commodities with high water content), kiwi, lemon, and orange (commodities with high acid content and high water content) [14]. All the matrices were purchased in organic quality in whole food shops. The samples were milled and homogenized under addition of dry ice. Subsequently, 10 g portions of the sample material were weighed into centrifuge tubes and frozen.

Two different extraction methods were tested: For non-buffered extraction, 10 mL of ACN were added to the frozen samples and the samples were shaken for 10 min using an overhead shaker (first extraction). Then, the extract was centrifuged (3000×*g*) for 5 min. For buffered extraction, a second extraction and phase separation followed. For this purpose, the contents of the Supel^{TM} QuE Citrate Extraction Tube were added to the obtained extract and the centrifuge tubes were shaken for 1 min. 600 µL of 5 M sodium hydroxide solution were added to lemon for pH adjustment. Then the extract was centrifuged (3000×*g*) for 5 min.

For all extraction methods, the supernatant was taken and transferred into vials for 2D-LC-Q-TOF-MS analysis. In case of investigations with spiked samples, the frozen samples were spiked with a mixture of analytes or, in case of blank tests, with the same amount of ACN. Each matrix was analyzed twice.

3. Results and discussion

3.1. Optimization of the HILIC method

It is important that the retention time difference (ΔRT) between the first and the last eluting analyte is as narrow as possible for ensuring that as few matrix components s as possible reach the RP column. The aim was to find the limits for such a window in order to allow a successive expansion of the multi-screening method without complex adjustment procedures. To determine ΔRT, all measurements were only carried out in the first dimension.

For these investigations, 135 analytes were chosen, covering a broad range of polarities (log K_{ow} −2.0 to 8.60) [15] and pK_a values (−1.5 to 15.70) [15,16]. An overview of these analytes and their log K_{ow} and pK_a values gives Table A in the Supporting information. The analytes were included in 10 mixtures and analyzed with the complete HILIC gradient. The eluents were prepared using phase combination 1 as recommended by JAS [13] (see Section 2.2.2.1). The analyte eluting the earliest was carbosulfan (retention time (RT) = 1.5 min) and nicotine eluted as the last analyte (RT = 6.5 min). For this reason, nicotine will not be detectable with the method settings and VST recommended by JAS [13]. Moreover, ΔRT expanded to 5.0 min with the chosen analytes. In comparison, the ΔRT of JAS was only 2.0 min [13]. Consequently, the HILIC method was optimized in order to obtain the lowest possible ΔRT.

3.1.1. Eluents with different pH values

The pH value of the mobile phase has a great impact on the ionization state of the analytes and therefore, in return, on their retention [17]. In this study two buffers, a 100 mM AF (pH = 3.2) and a 100 mM AA (pH = 5.8), were tested. These two pH values are recommended in the HILIC method development guidelines of Phenomenex [18]. The pH values represented in brackets refer to the buffer used to prepare the mobile phases, not to the eluent itself. For the studies, the eluents were prepared using phase combination 2 (compare to Section 2.2.2.1). This approach led to less RT shifts and a reproducible ΔRT. The measurements of the 135 analytes were carried out in both ESI modes.

Fig. 3 shows which analytes had the strongest influence on ΔRT for each ESI mode and each buffer. As obvious from example 1, ΔRT was 6.8 min in positive ESI mode with AA. Example 2 shows that ΔRT for AF was 6.9 min. It could be observed that the retention of nicotine and propamocarb changed significantly depending on the buffer. For nicotine, RT was 8.3 min with AF (example 2 in Fig. 3) and could be reduced to 4.1 min with AA. However, RT increased from 4.4 min (AF) to up to 8.0 min (AA) for propamocarb (example 1 in Fig. 3). ΔRT was 3.7 min (example 3 in Fig. 3) or 2.8 min (example 4 in Fig. 3) in negative ESI mode. Furthermore, it could be stated that the signal intensities were more intensive in negative ESI mode with AA, whereas the signal intensities were more intensive in positive ESI mode with AF. Therefore, method development was continued for negative ESI mode with AA and for positive ESI mode with AF in order to keep ΔRT as small as possible.

The investigations with the matrix components led to similar results. There were components like histamine, alliin, and tyramine, whose RT was influenced very strongly by a change of the buffer, or respectively, of pH value, whereas no shift in RT could be observed for other components (e.g., bergapten and β-carotene).

3.1.2. Column temperatures

Higher column temperatures were tested for optimizing ΔRT with 90 selected analytes. Tests at 30 °C, 40 °C, 50 °C and 60 °C were carried out. JAS recommended a temperature of 30 °C [13].

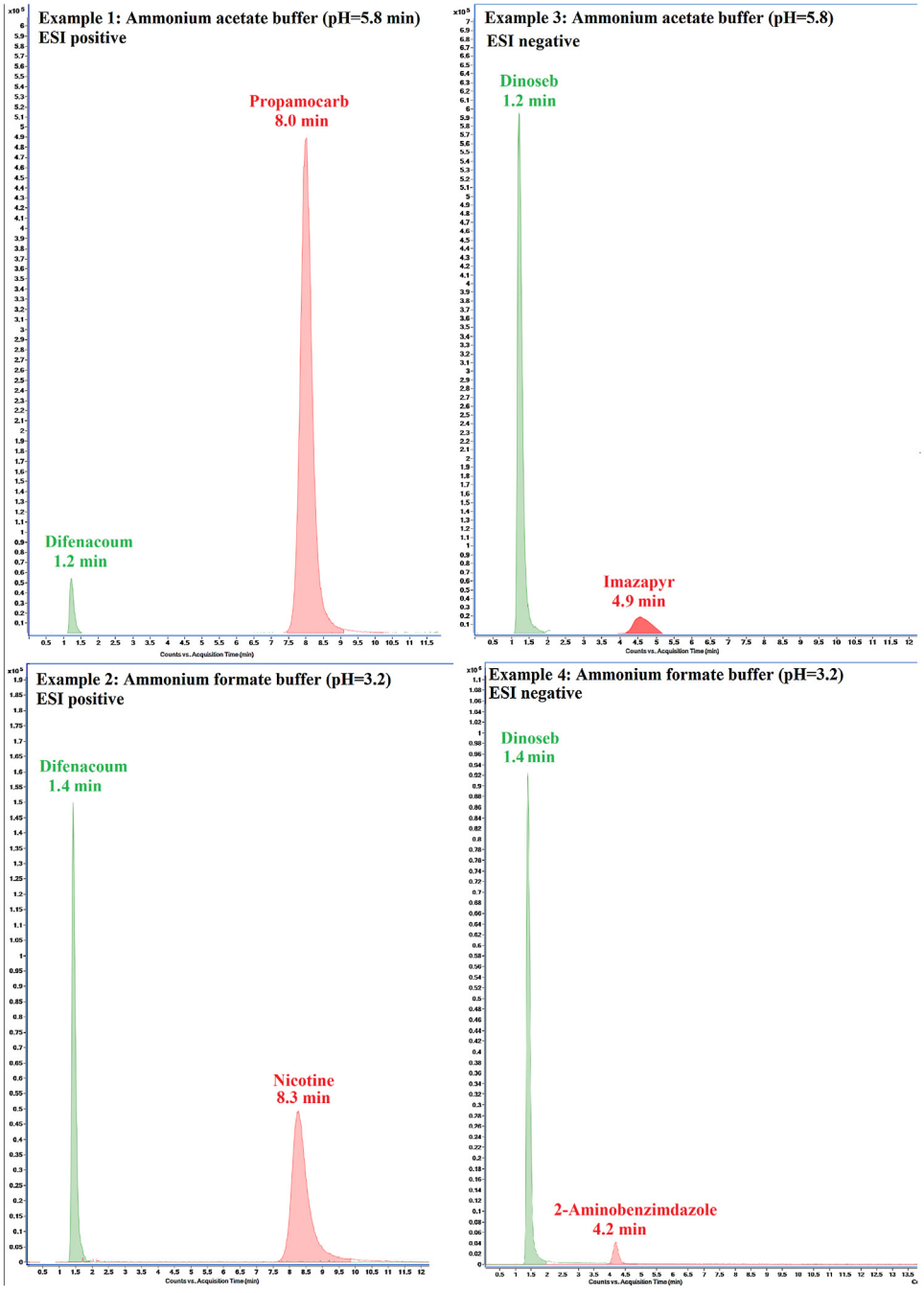

Fig. 3. Analytes that have the strongest influence on the ΔRT depending on the chosen buffer.

The measurements for these investigations were carried out with phase combination 2 and the two buffers.

In summary, it can be said that the increasing temperature diminished RT of most analytes. However, for some analytes no effect could be observed. The extent of decrease in RT was different for each analyte. It ranged from <0.1 min (difenacoum) to up to 3.6 min (nicotine) in positive ESI mode with AF (Table 2). The same could be observed in negative ESI mode and with AA: All RT decreased to a different extent, ranging from <0.1 min (hexaflumuron) to 2.5 min (imazapyr). Due to recommended temperature (20–40 °C) and lifetime of the HILIC column [19], it was decided to carry out all further investigations at a column temperature of 40 °C.

ΔRT was reduced from 6.9 min to 5.3 min in positive ESI mode and from 3.7 min to 2.7 min in negative ESI mode at 40 °C.

The measurement of the matrix components solutions at different temperatures confirmed the observations: All RT decreased to a different extent in both ESI modes. The RT shifts ranged from <0.1 min (bergapten) to 1.3 min (histamine).

Another apparent effect of elevated temperatures was that narrower peaks were obtained. The reason for this is the increased diffusion coefficient [20]. It was assumed that narrower peaks could be transferred to the second dimension more easily, because they are less vulnerable to splitting by valve switching.

Table 2
Adjusted ionization states of selected analytes depending on temperature.

Name	ESI mode	pH value	Temperature [°C]	RT [min]	Adjusted positive ionized [%]	Adjusted positive double ionized [%]	Adjusted non-ionized [%]	Adjusted negative ionized [%]
2.4.5-T	negative	5.8	30	1.97	0.00	0.00	0.11	99.89
2.4.5-T	negative	5.8	40	1.73	0.00	0.00	0.11	99.89
2.4.5-T	negative	5.8	50	1.67	0.00	0.00	0.11	99.89
2.4.5-T	negative	5.8	60	1.61	0.00	0.00	0.11	99.89
Difenacoum	positive	3.2	30	1.44	0.00	0.00	98.44	1.56
Difenacoum	positive	3.2	40	1.43	0.00	0.00	98.44	1.56
Difenacoum	positive	3.2	50	1.42	0.00	0.00	98.44	1.56
Difenacoum	positive	3.2	60	1.41	0.00	0.00	98.44	1.56
Difenacoum	negative	5.8	30	1.29	0.00	0.00	13.68	86.32
Difenacoum	negative	5.8	40	1.26	0.00	0.00	13.68	86.32
Difenacoum	negative	5.8	50	1.23	0.00	0.00	13.68	86.32
Difenacoum	negative	5.8	60	1.21	0.00	0.00	13.68	86.32
Forchlorfenuron	negative	5.8	30	1.62	0.00	0.00	100.00	0.00
Forchlorfenuron	negative	5.8	40	1.59	0.00	0.00	100.00	0.00
Forchlorfenuron	negative	5.8	50	1.58	0.00	0.00	100.00	0.00
Forchlorfenuron	negative	5.8	60	1.60	0.00	0.00	100.00	0.00
Fenpropidin	positive	3.2	30	2.67	99.68	0.00	0.32	0.00
Fenpropidin	positive	3.2	40	2.69	99.37	0.00	0.63	0.00
Fenpropidin	positive	3.2	50	2.65	98.76	0.00	1.24	0.00
Fenpropidin	positive	3.2	60	2.64	97.55	0.00	2.45	0.00
Flonicamid	negative	5.8	30	1.63	93.39	0.00	6.61	0.00
Flonicamid	negative	5.8	40	1.59	87.62	0.00	12.38	0.00
Flonicamid	negative	5.8	50	1.58	78.01	0.00	21.99	0.00
Flonicamid	negative	5.8	60	1.58	64.01	0.00	35.99	0.00
Formetanate	positive	3.2	30	3.93	90.91	0.00	9.09	0.00
Formetanate	positive	3.2	40	3.71	83.37	0.00	16.63	0.00
Formetanate	positive	3.2	50	3.43	58.55	0.00	41.45	0.00
Formetanate	positive	3.2	60	3.20	41.45	0.00	58.55	0.00
Nicotine	positive	3.2	30	8.28	99.30	0.56	0.14	0.00
Nicotine	positive	3.2	40	6.73	99.34	0.16	0.50	0.00
Nicotine	positive	3.2	50	5.61	96.91	0.03	3.07	0.00
Nicotine	positive	3.2	60	4.66	83.36	0.00	16.63	0.00
Propamocarb	positive	3.2	30	4.63	99.90	0.00	0.10	0.00
Propamocarb	positive	3.2	40	4.48	99.65	0.00	0.35	0.00
Propamocarb	positive	3.2	50	4.21	99.30	0.00	0.70	0.00
Propamocarb	positive	3.2	60	4.07	98.61	0.00	1.39	0.00
Pymetrozine	positive	3.2	30	2.53	0.03	0.00	99.97	0.00
Pymetrozine	positive	3.2	40	2.42	0.01	0.00	99.99	0.00
Pymetrozine	positive	3.2	50	2.30	0.00	0.00	100.00	0.00
Pymetrozine	positive	3.2	60	2.22	0.00	0.00	100.00	0.00
Quinclorac	positive	3.2	30	3.02	0.00	0.00	93.24	6.76
Quinclorac	positive	3.2	40	2.88	0.00	0.00	93.24	6.76
Quinclorac	positive	3.2	50	2.67	0.00	0.00	93.24	6.76
Quinclorac	positive	3.2	60	2.58	0.00	0.00	93.24	6.76
Spiroxamine	positive	3.2	30	2.66	16.63	0.00	83.37	0.00
Spiroxamine	positive	3.2	40	2.66	9.09	0.00	90.91	0.00
Spiroxamine	positive	3.2	50	2.60	4.77	0.00	95.23	0.00
Spiroxamine	positive	3.2	60	2.57	2.45	0.00	97.55	0.00

3.1.3. HILIC column materials

For these investigations, the measurements for 90 selected analytes were carried out with phase combination 2 at 40 °C. Kittlaus et al. [11] obtained the best results with a diol HILIC column (see column A in Section 2.2.2.1). As ΔRT was still very large after optimization of the temperature, it was decided to test further diol HILIC columns (columns B and C in 2.2.2.1).

No significant change of ΔRT could be observed with column B. Difenacoum eluted at 1.4 min and nicotine eluted at 5.8 min on column C in positive ESI mode. Therefore, ΔRT could be reduced from 5.3 min (column A) to 4.4 min (column C). Also in negative ESI mode, ΔRT decreased to 2.5 min with column C. For this reason, it was decided to use column C for all further investigations.

3.1.4. Buffer concentrations

An increase of the buffer concentration leads to a thicker water layer and affects the electrostatic interactions between charged analytes and charged stationary phases [17,21,22].

Therefore, the buffer concentration was increased from 5 mM to 10 mM for AF in positive ESI mode and for AA in negative ESI mode in this study. No significant change of ΔRT was observed in positive ESI mode. The higher buffer concentration increased RT for most of the analytes (increase by up to 0.3 min). A decreased RT by up to 0.2 min was observed for a few analytes. Again, nicotine was the analyte with the strongest influence on ΔRT. Therefore, ΔRT could only be reduced by 0.2 min to 4.2 min.

RT rose by 0.2–1.3 min for most of the analytes in negative ESI mode with the 10 mM AA. It was assumed that there was electrostatic repulsion between the charged acidic analytes and charged residual silanol groups of column C. All in all, ΔRT increased from 2.5 min (for 5 mM AA) to up to 3.8 min with the 10 mM AA.

Due to the small effect on ΔRT in positive ESI mode and the negative effect in negative ESI mode, it was decided to maintain the buffer concentration unchanged at 5 mM.

3.1.5. Flow rates

All previous measurements were carried out with a flow rate of 0.2 mL/min according to JAS [13]. Therefore, a higher flow rate of 0.3 mL/min was tested. The retention of all analytes decreased. Nicotine eluted at 4.0 min and difenacoum eluted at 0.9 min, result-

ing in a ΔRT of 3.1 min. Consequently, all further measurements were carried out with a flow rate of 0.3 mL/min. Also in negative ESI mode, a higher flow rate led to a decrease of all RT. Dinoseb was the first eluting analyte (RT = 0.8 min) and imazapyr was the last eluting analyte (RT = 3.0 min), resulting in a ΔRT of 2.2 min A decrease in RT could also be observed for matrix components when using a higher flow rate.

3.2. Influences on the elution behavior in HILIC

During optimization of ΔRT in the first dimension, it was observed that several analytes influenced ΔRT to different extents. This different eluting behavior during the whole optimization procedure was an impulse to elucidate which properties effected the elution of analytes in HILIC. It was decided to carry out further investigations in order to be able to estimate, whether new analytes will possibly expand the window within which the analytes elute from the HILIC column according to their pK_a values.

ΔRT was influenced by different buffer pH values and different analytes. The pH values mentioned in Section 3.1.1 refer to the buffers used when preparing the mobile phases. It was hypothesized that the ionization state of the analyte had a crucial influence. We tried to develop some kind of relation between RT and the ionization state of the analyte. The ionization state depends on both, the pK_a value of the compound and the pH value of the mobile phase. In turn, both are affected by the addition of organic solvent (in this case ACN) [21–25]. Consequently, when using organic solvents, the ionization state of compounds will be different from those in pure aqueous solutions [25]. In general, the pK_a value of acidic analytes increases with increasing ACN amounts, whereas the pK_a value of basic compounds decreases [24,25].

The ionization state (α) can be calculated according to the following formulas [24]:

$$\text{Bases}: \quad \alpha = \frac{1}{1 + 10^{pH - pka}} \tag{1}$$

$$\text{Acids}: \quad \alpha = \frac{1}{1 + 10^{pka - pH}} \tag{2}$$

It was decided to calculate the ionization state for several analytes that had the strongest influence on ΔRT. The Aim was to estimate, whether the ionization state was the reason for the elution behavior of the analytes depending on the mobile phase and the gradient.

At first, buffer pH values were adjusted to the ACN amount, according to literature data [23]. Kazakevich et al. [23] determined a pH shift from 0 to 60% of ACN for AA based on the studies of Espinosa et al. [26] and Canals et al. [27]. They found that the change depended on the starting pH value of the buffer, resulting in an upward pH shift of 0.3 units per 10% ACN for buffers with pH values of up to 6 [23]. There are no investigations regarding the change of pH values of AF.

Kazakevich et al. [23] determined that the pK_a values of basic analytes decreased by 0.2 units per 10% ACN (up to 50% of ACN). Kazakevich et al. [23] also determined the pK_a value shift of acidic analytes. It increased up to 0.3 units per 10% ACN (up to 35% ACN). We extrapolated the pK_a value shift of acids with published data of Espinosa et al. [28] and could confirm a pK_a value upward shift of 0.3 units per 10% ACN up to 60% ACN for acidic analytes. All these adjustments of pH and pK_a values work well for an organic content of up to 60% of ACN. Up to now, no further investigations have been carried out on the influence of higher ACN contents. For our purposes, we assumed that the described shifts in pH and pK_a values are valid for up to 90% of ACN. We have been aware that this is only an estimation.

The temperature has an influence on the pK_a value of the analytes, too. Increasing temperatures result in a downward shift of the pK_a value of basic analytes by 0.03 units per °C [23,29,30]. The pH value of acidic buffers and the pK_a value of acidic analytes are affected less strongly [23]. Therefore, we adjusted only the pK_a value of the basic analytes to the temperature. Table B in the Supporting information gives an overview of the adjustments of pH and pK_a values.

Based on the adjusted pK_a and pH values, the ionization states of the analytes were calculated at hand of Formulas (1) or (2). First, a certain RT range was assigned to a specific ACN content based on eluent composition and the HILIC gradient. For example, the range from 0 to 2.5 min was assigned to 90% of ACN. On the basis of the ACN content and the temperature, the pK_a values of the analytes and the pH value of the buffer were adjusted as described above. After this, the ionization states for the analytes were calculated. Table 3 shows the adjusted ionization states of exemplary analytes (the unadjusted ionization states are shown in brackets). The pK_a values were taken from the Pesticide Manual [31], EURL-DataPool [15], approval documents (if available), or further literature. If there was no reference, the pK_a values were calculated using ACD/Labs Percepta software [16].

3.2.1. Influence of buffer pH value

Two buffers with different starting pH values (AF = pH 3.2 and AA = pH 5.8) were tested. At first, measurements with both buffers were carried out in both ESI modes. Table 3 shows the adjusted ionization states of exemplary analytes and the relevant ESI mode. As obvious from Table 3, RT is the same with both buffers for bromacil, carbendazim, isomethiozin, and pirimicarb. The reason is that these analytes were not ionized at either of the two pH values. Without adjusting the pH/pK_a value, carbendazim and pirimicarb would have been ionized >90% at pH 3.2 and <4% at pH 5.8. As both would be ionized to a higher degree at pH 3.2, they should have a higher RT than at pH 5.8. The actual elution behavior of these analytes would be difficult to explain without the pH/pK_a value adjustment.

Dinoseb, formetanate, nicotine, and spinosyn A had a lower RT at pH 5.8 than at pH 3.2. These analytes were ionized to a lower degree at pH 5.8, and are therefore less polar. Without the pH/pK_a value adjustment, the ionization state of formetante and spinosyn A would not change at any of the two pH values. This means that both substances should have the same RT at both pH values. These are further examples go to show that the adjustment seems to be a good model for explaining the elution behavior.

4-CPA, difenacoum, and propamocarb are examples that indicate that the ionization state of the analyte is not the only factor influencing the retention. RT is the same for 4-CPA at both pH values in negative ESI mode, even though its ionization state was significantly higher at pH 5.8. Usually, RT should be higher at pH 5.8 due to the higher polarity.

RT was lower for difenacoum at pH 5.8 than at pH 3.2 (RT shift = 0.2 min), even though its ionization state was significantly higher at pH 5.8. Difenacoum should be more polar in its ionized state, therefore RT should be higher at pH 5.8.

The ionization state of propamocarb was nearly the same at both pH values, but its RT was significantly higher at pH 5.8 than at pH 3.2 (RT shift = 3.4 min).

Usually, the RT should be the same due to the similar polarity. A possible explanation for these examples may be the electrostatic interaction between analyte and stationary phase. Diol columns rank among the neutral stationary phases, because the functional groups are not charged in the typically used pH range [21]. However, it is possible that the residual silanol groups of diol columns carry negative charges at a pH value above 4–5 due to deprotonation [17,21]. Therefore, deprotonated residual silanol groups may lead to electrostatic interactions [17]. In case of propamocarb, the

Table 3
Adjusted ionization states of selected analytes. The unadjusted ionization states are presented in brackets.

Name	ESI mode	pH value	Temperature [°C]	RT [min]	Adjusted positive ionised [%]	Adjusted positive double ionised [%]	Adjusted non-ionised [%]	Adjusted negative ionised [%]
4-CPA	negative	3.2	30	2.4	0.00	0.00	69.61 (69.61)	30.39 (30.39)
4-CPA	negative	5.8	30	2.4	0.00	0.00	0.57 (0.57)	99.43 (99.43)
Bromacil	negative	3.2	30	1.7	0.00	0.00	100.00 (100.00)	0.00
Bromacil	negative	5.8	30	1.7	0.00	0.00	99.97 (99.97)	0.03 (0.03)
Carbendazim	positive	3.2	30	1.9	0.02 (90.91)	0.00	99.98 (9.09)	0.00
Carbendazim	positive	5.8	30	1.9	0.00 (2.45)	0.00	100.00 (97.55)	0.00
Difenacoum	positive	3.2	30	1.4	0.00	0.00	98.44 (98.44)	1.56 (1.56)
Difenacoum	positive	5.8	30	1.2	0.00	0.00	13.68 (13.68)	86.32 (86.32)
Dinoseb	negative	3.2	30	1.4	0.00	0.00	6.20 (6.20)	93.80 (93.80)
Dinoseb	negative	5.8	30	1.2	0.00	0.00	96.34 (96.34)	3.66 (3.66)
Formetanate	positive	3.2	30	3.9	90.91 (100.00)	0.00 (0.00)	9.09 (0.00)	0.00
Formetanate	positive	5.8	30	2.7	0.79 (99.50)	0.00 (0.00)	99.21 (0.50)	0.00
Isomethiozin	positive	3.2	30	1.5	0.00 (0.60)	0.00	100.00 (99.40)	0.00
Isomethiozin	positive	5.8	30	1.5	0.00	0.00	100.00 (100.00)	0.00
Nicotine	positive	3.2	30	8.3	99.30 (55.73)	0.56 (44.27)	0.14 (0.00)	0.00
Nicotine	positive	5.8	30	4.1	5.32 (99.40)	0.00 (0.20)	94.68 (0.40)	0.00
Pirimicarb	positive	3.2	30	1.6	0.04 (94.06)	0.00 (0.00)	99.96 (5.94)	0.00
Pirimicarb	positive	5.8	30	1.6	0.00 (3.83)	0.00 (0.00)	100.00 (96.17)	0.00
Propamocarb	positive	3.2	30	4.6	99.90 (100.00)	0.00	0.10 (0.00)	0.00
Propamocarb	positive	5.8	30	8.0	97.81 (99.98)	0.00	2.19 (0.02)	0.00
Spinosyn A	positive	3.2	30	2.7	75.97 (100.00)	0.00	24.03 (0.00)	0.00
Spinosyn A	positive	5.8	30	2.4	0.44 (99.50)	0.00	99.56 (0.50)	0.00

elution was retarded because of the attraction between the positively charged analyte and the negatively charged residual silanol groups.

4-CPA and difenacoum were negatively charged analytes and eluted earlier, because the deprotonated residual silanol groups caused analyte repulsion. In case of negatively charged analytes the retardation, due to higher polarity and the repulsion, effected by the residual silanol groups would counteract each other. This can be noted when negatively charged analytes showed the same or a lower retention time at pH 5.8 than negatively charged analytes at pH 3.2 (e.g., 4-CPA and difenacoum in Table 3).

The YMC-Pack Diol-HILIC and YMC-Triart Diol-HILIC columns were not endcapped. We assumed that, as a consequence of the adjustments, pH values will increase from 3.2 to 5.9 and from 5.8 to 8.5, respectively. This means that the residual silanol groups will be deprotonated at both pH values. However, the pK_a value of the residual silanol groups will also be affected. Nevertheless, there are no studies about the influence of ACN on the deprotonation of residual silanol groups. These findings indicate that the deprotonation of the residual silanol groups shifts to higher pH values. It is possible that the residual silanol groups are partly deprotonated at pH 3.2 and 5.9, respectively. Nevertheless, their influence on the analytes' elution seems to be stronger at pH 5.8 and 8.5, respectively.

It was further tested, whether the model could be used to estimate if new analytes or matrix components will elute within or outside the window. Therefore, the adjusted ionization states were calculated for some matrix components that are similar to the basic analytes that have the greatest influence on ΔRT (e.g., nicotine). Thus, it was aimed at investigating the matrix separation simultaneously. In the following, the approach and results for histamine are described. We calculated the ionization state adjusted to the eluent composition (90% of ACN). Under these conditions, histamine is ionized about 97% with AF and is non-ionized about 91% with AA. We assumed that histamine would expand ΔRT more than nicotine, because of its higher pK_a value. Consequently histamine, as polar matrix component, may be separated in HILIC (measurement of the polar analytes ends after elution of nicotine).

In order to prove this, we repeated the measurement of histamine at both pH values in the first dimension and could confirm the initial assumption. Histamine eluted at 12.2 min with AF and at 3.8 min with AA. We calculated the ionization states with the determined RT, adjusted to the relevant ACN content. Histamine is very polar in AF, because it is double ionized to a degree of approximately 71% and single ionized to a degree of 29%. However, it is only single ionized to a degree of 36% in AA and is therefore less polar. This could be the reason for the intense RT shift, depending on the pH value. The model worked well for tyramine, too.

3.2.2. *Influence of column temperature*

It should be noted that we use AF for the tests in positive ESI mode with pH 3.2 and AA for the tests in negative ESI mode with pH 5.8. We supposed that with increasing temperature, the ionization state of basic analytes was decreased and therefore, the analytes were less polar and eluted earlier in positive ESI mode with AF. To verify this, we adjusted the pK_a values of selected analytes depending on the column temperature and calculated the ionization state for AF and AA. However, we did not adjust the pH value of the mobile phase, because we could not find any studies describing the influence of temperature on amphoteric buffers.

All in all, the increasing temperatures led to a decreased RT for most analytes in both ESI modes. Table 2 shows the adjusted ionization states for selected analytes depending on temperature.

No significant shifts in RT (<0.1 min) could be observed for most of the analytes that are not ionized at any temperature. Such analytes are, for example, difenacoum (positive ESI mode) and forchlorfenuron (negative ESI mode). However, there were exceptions in positive ESI mode. A closer look at the acidic analytes illustrates that quinclorac behaves differently. Although it is non-ionized about 90%, the RT shift is >0.4 min with increasing temperature. Looking at the basic analytes, there are also non-ionized analytes (e.g., pymetrozine), whose RT shifts are >0.3 min. This could not be observed in negative ESI mode.

Our assumption that the ionization state as well as RT decrease with increasing temperature could be confirmed for some basic analytes measured in positive ESI mode. For example, this applies to formetanate. We observed that some basic analytes (e.g., flonicamid) showed a decreased ionization in negative ESI mode, but their RT shifts are <0.1 min. We assumed that this was due to the attractive interactions of the residual silanol groups with the still ionized analytes.

We observed for both buffers or in both ESI modes, respectively, that the polar analytes which elute later (after 2.0 min) (e.g., nico-

tine and propamocarb) were affected more strongly by increasing temperatures. Mostly, these analytes were ionized. For example, propamocarb was ionized to a degree of 99% at all temperatures with AF, and although its ionization state did not change, the RT shift was >0.6 min. For example, 2,4,5-T, was almost completely ionized with AA at all temperatures and its RT shift was >0.3 min. However, the ionization state was not the only explanation for the greater influence of the temperature. There were ionized analytes whose RT did not shift. These were, for example, fenpropidin in positive ESI mode or difenacoum in negative ESI mode. A reason, why especially the polar analytes are influenced by temperature could be that elevated temperatures weaken the hydrogen bonding [32,33]. Furthermore, the transfer of hydrophilic analytes from the hydrophobic acetonitrile phase to the hydrophilic water layer on the stationary phase is an exothermic process. Therefore, it is favoured by lower temperatures [17,32,33].

The investigations with matrix components showed the same tendencies. Non-ionized compounds (e.g., bergapten, β-carotene) were affected less strongly than ionized compounds. In general, the polar and late eluting matrix components like histamine and tyramine in positive ESI mode and nicotinic acid in negative ESI mode, were strongly influenced by increasing temperatures. However, this also applied to hesperidin in positive ESI mode, although this compound was non-ionized.

For most analytes, the statement of Kazakevich and LoBrutto [23] was confirmed that basic compounds with $pK_a > 6$ undergo the greatest influence of temperature. However, there were also exceptions. Some basic analytes with $pK_a > 6$ (spiroxamine, fenpropidin and flonicamid) were not influenced by temperature, and in turn, basic analytes with pK_a values < 6 (cymiazole, cyromazine, cotinine and pymetrozine) were strongly influenced by temperature. An explanation may be the accuracy of the pK_a values. In some cases a broad range of pK_a values exists in literature for a single substance. It is difficult to determine the "correct" one. Another explanation may be that there is an effect of temperature on the pK_a value of the residual silanol groups, the amphoteric buffer, and acidic compounds. There are no studies about these issues that describe the range of changes.

3.2.3. Influence of buffer concentration

There was no significant influence of the buffer concentration on ΔRT in positive ESI mode. However, there was a negative effect in negative ESI mode with the 10 mM AA, as RT was increased for most analytes. An increase of RT between 0.2 and 1.3 min could be observed for all negatively charged analytes. For example, RT was increased by 0.6 min for 4-CPA. The ionization state was calculated again with the adjusted parameters. The increase in RT with a higher buffer concentration suggests that there are residual silanol group activities. Due to the higher buffer concentration, the deprotonated residual silanol groups are shielded by the buffer salts. Therefore, the electrostatic repulsion is weakened, leading to an increased retention.

However, RT of non-ionized analytes was not influenced by a higher buffer concentration (e.g., fuberidazole).

3.2.4. Influence of flow rate

We could observe that the influence of the flow rate was much stronger on the polar analytes that eluted later (after 2.0 min). RT of these analytes decreased by 0.7 to up to 2.2 min in positive ESI mode and by 0.6 to up to 0.8 min in negative ESI mode. The decrease in RT of the less polar and non-ionized analytes was by 0.4 to up to 0.6 min in positive ESI mode and by 0.3 to up to 0.5 min in negative ESI mode. It can be assumed that the higher flow rate shifts the analytes that elute after 2.5 min to earlier RT and therefore, to higher ACN contents. This in turn leads to less ionization, whereby the retardation is further decreased. However, this could only be observed for some individual analytes such as 2-aminobenimidazole and spinosyn A/D.

We could also confirm the effect that the polar analytes are influenced more strongly by the measurement of matrix components. For example, histamine, nicotinic acid, and tyramine were late eluting components (eluting from 3.7 to 11.3 min) in positive ESI mode and their RT decreased by at least 0.7 min. The greatest effect occurred for histamine. Its RT decreased from 11.3 to 8.8 min with increasing flow rate. The same effect was observable in negative ESI mode. The effect on the non-polar non-ionized matrix components was small in comparison (RT shift <0.5 min).

3.2.5. HILIC parameters

We determined the following HILIC parameters to be optimal: column C with phase combination 2 and 5 mM buffer (AA for negative ESI mode and AF for positive ESI mode), a flow rate of 0.3 mL/min and a column temperature of 40 °C.

With these parameters, the window was 3.1 min in positive ESI mode (the first/last eluting analytes were difenacoum and nicotine) and 2.2 min in negative ESI mode (the first/last eluting analytes were dinoseb and imazapyr).

3.3. Determination of valve switching times

3.3.1. Positive ESI mode

For this purpose, we chose 44 of the already measured analytes that had the strongest influence on ΔRT with AF. RT of these analytes determined during optimization of the first dimension were used as orientation for the determination of the VST.

Difenacoum was the first eluting analyte (RT = 0.9 min) under these conditions, therefore valve 1 had to switch to position A before difenacoum eluted from the HILIC column (initiation of state II (trapping phase), compare Fig. 1). Valve 2 switched to position A immediately after valve 1 switched for water addition. The determination of the switching times for valve 1 and 2 in position A were relatively easy. By contrast, the determination of the switching time for valve 2 in position B (initiation of state III (measurement of polar analytes), compare Fig. 1) was determined by extensive testing. When valve 2 switched too early, the analyte (e.g., thiabendazole and chlordimeform) could not be enriched on the trap and was transferred directly to the Q-TOF-MS.

When valve 2 switched too late, the more polar analytes (e.g., methamidophos and monocrotophos) broke through the trap column. The switching of valve 1 to position B initiates the start of the RP measurement. This means that valve 1 has to switch after elution of the last analyte from the HILIC column (here: nicotine RT = 4.0 min).

Our intention was not to specify the VST without splitting the analytes. We aimed at enriching as many analytes as possible on the trap column. Therefore, it was acceptable, if one analyte was partly measured on the HILIC column and partly on the RP column. Our focus laid on screening and not on quantitative determination.

The VST were optimal when as many analytes as possible were fully trapped, as little analytes as possible were split and analyte(s) did not break through the trap column. Various combinations of VST were tested for these investigations. The best results were obtained with the VST shown in column 5 of Table 1. With these VST, it was possible to trap 23 out of the 44 analytes (9 were split), and 21 analytes were transferred directly to the Q-TOF-MS.

3.3.2. Negative ESI mode

Thirty-four analytes that had the strongest influence on ΔRT with AA were used for the determination of the VST. RT of these analytes were determined during ΔRT optimization. The VST found to be optimal for negative ESI mode are shown in column 6 of Table 1. With these VST, it was possible to trap 22 analytes out

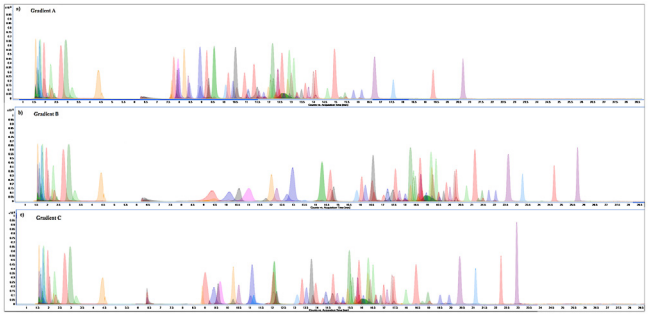

Fig. 4. Comparison of the elution profiles of 135 analytes with three different RP gradients.

of the 34 analytes (1 was split), and 12 analytes eluted directly to the Q-TOF-MS.

3.4. Optimization of the RP method

3.4.1. Test of RP gradients

We tested gradient A (based on the gradient of JAS [13], gradient B (based on the gradient of our existing screening method [12]) and five other gradients (including gradient C). 135 analytes were used to evaluate the elution profile and separation of the analytes depending on the different gradients. The peak shape of the very polar analytes (6.0–7.0 min) was very broad with gradient A and most of the analytes eluted in the range of 7.5–14.0 min. The last analyte eluted at 20.7 min. With gradient B, the analytes eluted in a wider range (9.0–20.5 min). This is better for developing a multi-method, because the peaks are distributed more evenly. The last analyte eluted at 25.7 min. However, the analytes eluted as wide peaks between 6.0 min and 13.0 min. We tested five further gradients in order to reach better peak shapes for those analytes. Gradient C was the optimal one. The relevant analytes showed narrower and more intensive peaks in the range of 6.0 min – 11.5 min. Therefore, gradient C was chosen. Fig. 4 shows the analytes' elution profiles for the three gradients.

3.4.2. Test of RP columns

Another point of optimization was the RP-column. JAS [13] and Kittlaus [11] et al., respectively, used an Agilent Poroshell 120 EC-C18 column (2.1 mm × 100 mm, 2.6 μm; 100 Å). The C-18 material was used, because in theory all very polar compounds are separated by HILIC and only the non-polar analytes are separated by RP. However, there are also differences in polarity of the non-polar analytes. For example, oxydemeton-methyl, carbendazim, and monocrotophos are the most polar analytes eluting on RP. Therefore, we decided to test column A, *i.e.* an RP-C18 column with polar groups on the surface. For comparison purposes, we used other RP-C18 columns (see column B and column C in Section 2.2.3.1). Furthermore, measurements were carried out with a column length of 150 mm. In comparison to columns B and C, the analytes eluted over a wider and more even range on column A. Additionally, the most polar analytes eluted as narrower and taller peaks. Fig. 4c) shows the elution profiles of 135 analytes with gradient C on column A.

We decided to test column D, because it was a Poroshell column by Agilent with polar groups on the C18 surface. We thought that this column should have a similar effect as column A. However, this column did not bring the desired success. Column A still delivered the best results with regard to peak shape of the most polar analytes. Therefore, we decided to carry out further measurements with column A.

3.5. Scope extension of the optimized method

The method of JAS includes 310 analytes and only six out of those analytes are transferred directly to the Q-TOF-MS [34]. We measured 275 further analytes to verify the chosen VST with the optimized parameters in both ESI modes. Consequently, our complete method contains 410 analytes including 193 new analytes in comparison to JAS. Thirty-five out of these 410 analytes are transferred directly to the Q-TOF-MS and 375 analytes are trapped and measured by means of RP. Only 23 analytes are trapped partly.

3.6. Influence of VST on matrix components

To investigate the influence of the VST on matrix components and with regard to matrix separation, we measured a mixture of matrix components (see Chapter 2.2.2.3) with the optimal VST.

Some matrix components are very polar (e.g., histamine, compare to Section 3.2.1). These components were retained to a high degree on HILIC and therefore elute after the last eluting analyte (nicotine or imazapyr). For example, nicotinic acid eluted at 3.8 min in negative ESI mode. These polar matrix components were transferred directly to the waste with the optimal VST and thus do not interfere with the analytes' detection. In other words, the very polar matrix components were not detectable. Polar matrix components that can be separated by HILIC included histamine, tyramine, and alliin in positive ESI mode and nicotinic acid in negative ESI mode.

However, other matrix components eluted within the window and thus may interfere with the analytes' detection. For example, hesperidin was measured directly via HILIC, whereas hesperitin and bergapten were trapped and transferred to RP.

3.7. Optimization of sample preparation

JAS [13] recommends to weigh 10 g of homogenized sample material into centrifugation tubes for aqueous and acidic matrices like fruit and vegetables. Then, 100 μL of internal standard with a concentration of 1 ppm and 9.9 mL of ACN were added and vortexed vigorously for 10 min. After this, the samples were centrifuged at 3000×*g* for 5 min and the supernatant is filled into vials. In some cases, a phase separation of ACN and water can occur [13]. This was observed for the tested matrices beetroot and kiwi. Reasons for the phase separation may be the high sugar content in kiwi and the pigments in beetroot. In these cases, it is recommended to proceed with the ACN phase, as the use of the internal standard should compensate for the error [13].

The question arose, whether the injection of a water/ACN mixture affected the elution of the analytes. Furthermore, the use of the QuEChERS citrate salts is useful for phase separation, pesticide partitioning and pH adjustment. Citrate buffering ensures a complete extraction of acidic pesticides and the protection of acid- or base-labile analytes [4]. Furthermore, we do not want to rely on the partitioning of an internal standard when using a method with such a high number of analytes. Therefore, we tested a QuEChERS-based extraction. To compare the two extraction methods, blank matrices were prepared as described in Section 2.3. The extraction recommended by JAS [13] corresponds to non-buffered, and the QuEChERS-based extraction corresponds to buffered extraction. For a better comparability, the blank matrices were spiked with the pesticide mixture in such a way that the on-column concentration was the same for both extractions. Comparing both extraction methods, it could be recognised that the peak shape of several analytes was affected negatively without the phase separation by injection of the water/ACN mixture. For some analytes, broad and split peaks occurred. Fig. 5 shows the comparison of the extraction methods on the basis of the peak shapes of two selected analytes.

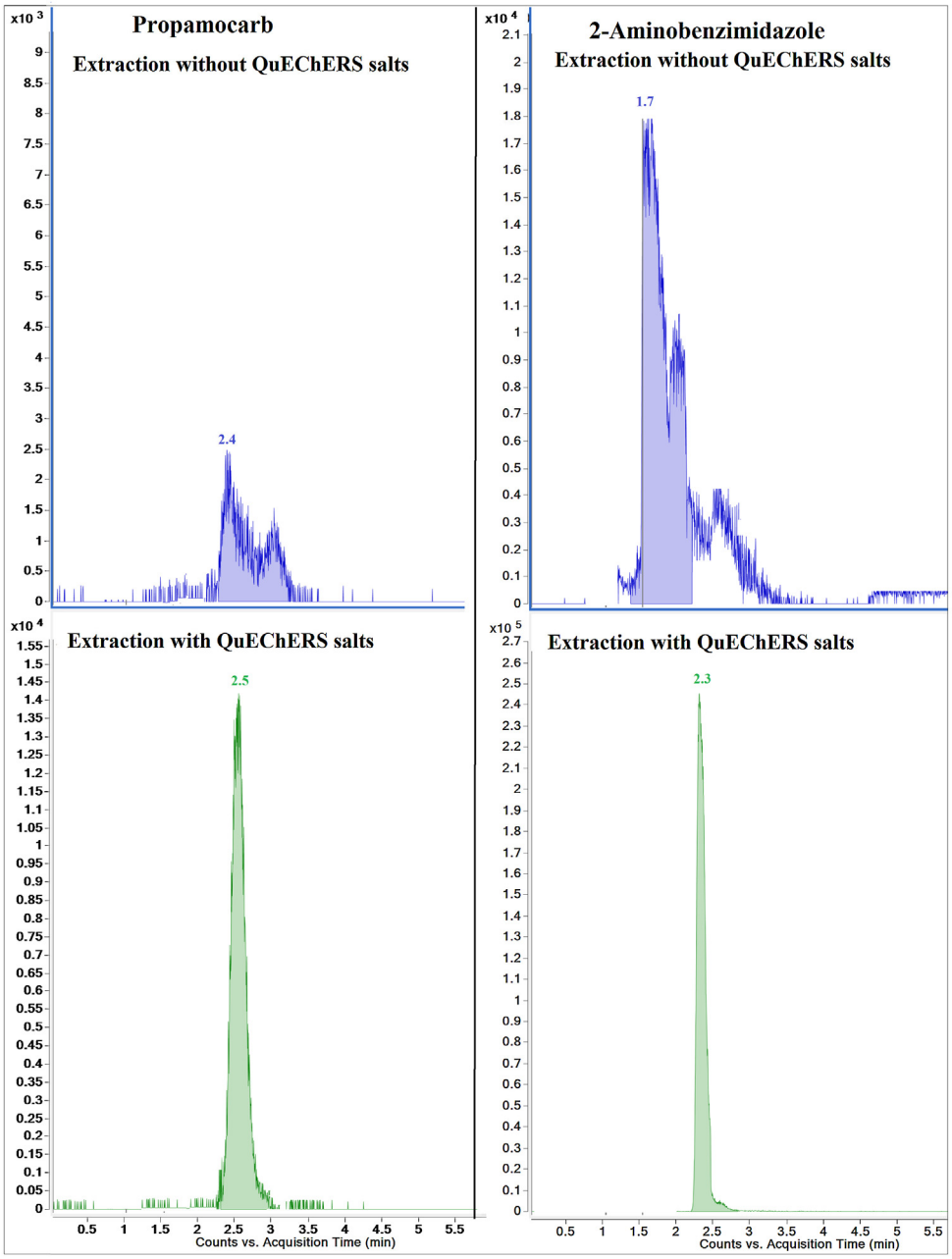

Fig. 5. Comparison of the extraction methods with and without QuEChERS salts on the basis of two selected analytes.

We excluded the matrices beetroot and kiwi from the comparison, because of the phase separation occurring in both extraction methods. For the matrix cucumber, we observed that 13 analytes produced better peak shapes with buffered extraction and only four analytes produced better peak shapes with non-buffered extraction. This applied to all analytes that are measured directly by means of HILIC. In total, eleven analytes could be detected better with buffered extraction, while these analytes could not be detected in certain matrices with non-buffered extraction. For the matrix beetroot, we observed another positive side effect of the QuEChERS salts. Also the pigments precipitated and clear colourless extracts were obtained. In contrast, no phase separation occurred without the use of citrate salts and both phases were intensively coloured. We decided to use the buffered extraction because of the reproducible phase separation, the better peak shapes of the polar analytes, the better detection rate and the additional matrix separation. Fig. 6 shows the workflow of the sample preparation and the optimized 2D-LC parameters.

3.8. Test of different injection volumes

An advantage of HILIC in contrast to RP is that sample extracts in pure ACN can be directly injected without evaporation or reconstitution [33]. Furthermore, it is possible to inject larger volumes. Therefore, we decided to test larger injection volumes. We injected 8 μL, 15 μL, 20 μL, 30 μL, and 40 μL of pure standard mixtures in ACN and spiked matrix extracts for comparison. The peaks broadened and the intensity increased with increasing injection volume. In some cases, the peak widths broadened extremely. For some analytes, the peaks splitted at an injection volume of 30 μL. However, for most analytes, no negative effects could be observed. The same

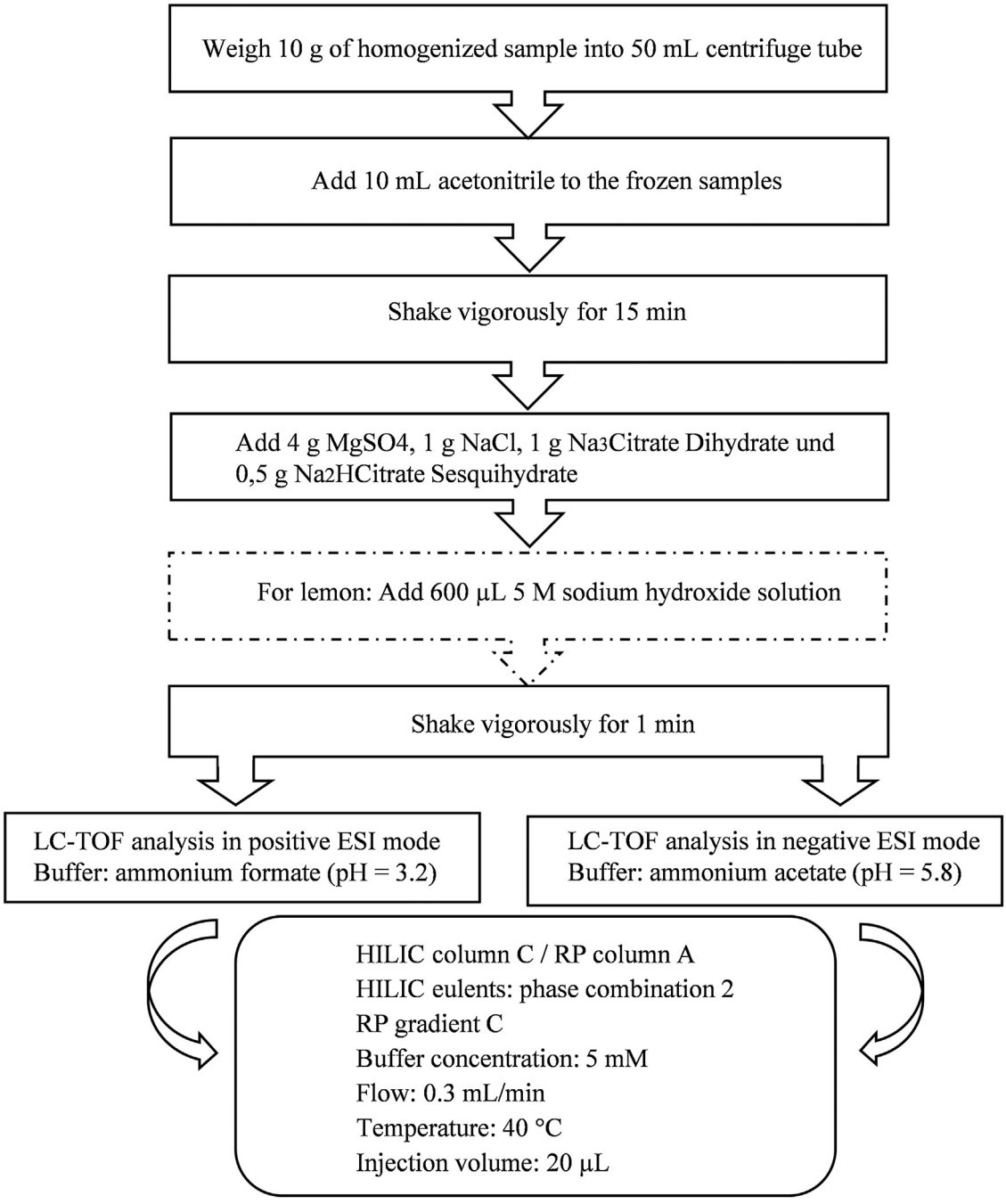

Fig. 6. Workflow of the sample preparation and optimized 2D-LC parameters.

observation could be made during the tests with spiked matrix extracts. The signal intensities of some analytes were saturated at an injection volume of 30 µL in the matrix beetroot. However, an identification was still possible. We decided to use an injection volume of 20 µL, although it is possible to use higher injection volumes.

4. Conclusions

In this study, a fully automated 2D-LC-system coupled to a Q-TOF-MS was evaluated for pesticide analysis. To our knowledge, this is the first time that a 2D-LC system is coupled to a Q-TOF-MS and used for a pesticide multi-screening approach. It was investigated, whether this system was applicable as a full-scan multi-screening method. We observed that the window within which the analytes eluted in the first dimension, expanded too far, and therefore optimized the separation(s).

The complete optimized method contains 410 analytes, including 193 new analytes in comparison to the JAS protocol. Thirty-five out of these 410 analytes are transferred directly to the Q-TOF-MS, and 375 analytes are trapped and measured via RP. Only 23 analytes are trapped partly. As the focus laid on screening, it was acceptable, when one analyte was partly measured on the HILIC column and partly on the RP column (splitted peaks). Furthermore, it will be easier to successively expand the method with this approach. However, we think it is possible to quantitatively determine the split analytes by summing up the areas of the two parts of the peak. This

hypothesis will be part of further studies. The results show that the optimized VST are suitable to successively expand the scope of the method without time-intensive adjustments of the VST.

It could be observed that the window was influenced by different buffer pH values and different analytes. To find an explanation, we adjusted the pH value of the mobile phase and the pK_a value of the analytes to the ACN content and temperature. As a next step, we calculated the ionization states of the analytes. We could determine that the pH-depending RT shift could be explained better with the adjustment. We are aware that this adjustment is only an estimation. Nevertheless, the model provides a good explanation for the elution behavior of the measured analytes and can be a tool for estimating the polarity, and therefore, the elution behavior (e.g., within or outside the window) of new analytes.

It can be noted that the ionization state has a great influence on the analytes' RT. The flow rate and temperature influence the analytes' RT to different extents. However, polar analytes are influenced more strongly than non-polar analytes.

An advantage of the 2D-LC approach is that there exist no cleanup options for different matrices as in comparison to QuEChERS. Therefore, the possible loss of analytes due to unsuitable options is minimized. In this study, the sample extraction was modified. Citrate salts for better extraction, reproducible phase separation, and pH adjustment were used. For selected polar matrix components, we could show separation from the analytes by HILIC. It seems that the system is equal or may be even better than QuEChERS. Nevertheless, further investigations using spiked matrices have to follow.

Acknowledgements

The authors thank Joint Analytical Systems GmbH (Moers, Germany) for support and providing the EPICS.

Appendix A. Supplementary data

Supplementary material related to this article can be found, in the online version, at doi:https://doi.org/10.1016/j.chroma.2019.04.003.

References

[1] O. Strubelt, Gifte in Natur und Umwelt: Pestizide und Schwermetalle, Arzneimittel und Drogen, 1st ed., Spektrum Akademischer Verlag, Heidelberg, Berlin, Oxford, 1996.
[2] K. Haider, A. Schäffer, Umwandlung und Abbau von Pflanzenschutzmitteln in Böden, 1st ed., Enke, Stuttgart, 2000.
[3] M. Anastassidades, S.J. Lehotay, D. Stajnbaher, F.J. Schenck, Fast and easy multiresidue method employing acetonitrile extraction/partitioning and dispersive solid-phase extraction for the determination of pesticide residues in produce, J. AOAC Int. 86 (2003) 412–431.
[4] P. Paya, M. Anastassidades, D. Mack, I. Sigalova, B. Tasdelen, J. Oliva, A. Barba, Analysis of pesticide residues using the quick easy cheap effective rugged and safe (QuEChERS) pesticide multiresidue method in combination with gas and liquid chromatography and tandem mass spectrometric detection, Anal. Bioanal. Chem. 389 (2007) 1697–1714, http://dx.doi.org/10.1007/s00216-007-1610-7.
[5] P. Jandera, Stationary phases for hydrophilic interaction chromatography, their characterization and implementation into multidimensional chromatography concepts, J. Sep. Sci. 31 (2008) 1421–1437, http://dx.doi.org/10.1002/jssc.200800051.
[6] P. Dugo, F. Cacciola, T. Kumm, G. Dugo, L. Mondello, Comprehensive multidimensional liquid chromatography: theory and applications, J. Chromatogr. A 1184 (2008) 353–368, http://dx.doi.org/10.1016/j.chroma.2007.06.074.
[7] W. Jian, R.W. Edom, Y. Xu, N. Weng, Recent advances in application of hydrophilic interaction chromatography for quantitative bioanalysis, J. Sep. Sci. 33 (2010) 681–697, http://dx.doi.org/10.1002/jssc.200900692.
[8] F. Cacciola, D. Giuffrida, M. Utczas, D. Mangraviti, P. Dugo, D. Menchaca, E. Murillo, L. Mondello, Application of comprehensive two-dimensional liquid chromatography for carotenoid analysis in Red Mamey (Pouteria sapote) fruit, Food Anal. Methods 9 (2016) 2335–2341, http://dx.doi.org/10.1007/s12161-016-0416-7.
[9] X. Wang, S.M.C. Buckenmaier, D. Stoll, The growing role of two-dimensional LC in the biopharmaceutical industry, J. Appl. Bioanal. 3 (2017) 120–126, http://dx.doi.org/10.17145/jab.17.015.
[10] S. Granafei, P. Azzone, V.A. Spinelli, I. Losito, F. Palmisano, T.R.I. Cataldi, Hydrophilic interaction and reversed phase mixed-mode liquid chromatography coupled to high resolution tandem mass spectrometry for polar lipids analysis, J. Chromatogr. A 1477 (2016) 47–55, http://dx.doi.org/10.1016/j.chroma.2016.11.048.
[11] S. Kittlaus, J. Schimanke, G. Kempe, K. Speer, Assessment of sample cleanupand matrix effects in the pesticide residue analysis of foods using postcolumninfusion in liquid chromatography–tandem mass spectrometry, J.Chromatogr. A 1218 (2011) 8399–8410, http://dx.doi.org/10.1016/j.chroma.2011.09.054.
[12] S. Muehlwald, N. Buchner, L.W. Kroh, Investigating the causes of low detectability of pesticides in fruits and vegetables analysed by high-performance liquid chromatography – time-of-flight, J. Chromatogr. A 1542 (2018) 37–49, http://dx.doi.org/10.1016/j.chroma.2018.02.011.
[13] Instruction Manual EPICS - Version 1.05, Joint Analytical Systems GmbH, 2015.
[14] Document No. SANTE/11813/2017, Guidance document on analytical quality control and validation procedures for pesticide residues analysis in food and feed, https://ec.europa.eu/food/sites/food/files/plant/docs/pesticides_mrl_guidelines_wrkdoc_2017-11813.pdf. (Accessed 1 August 2018).
[15] EURL-DataPool. https://www.eurl-pesticides-datapool.eu. (Accessed 21 May 2018).
[16] ACD/Labs Percepta software, Version 2017.2.1, 2017.
[17] G. Greco, T. Letzel, Main Interactions and Influences of the Chromatographic Parameters in HILIC Separations, J. Sep. Sci. 51 (2013) 684–693, http://dx.doi.org/10.1093/chromsci/bmt015.
[18] Guidelines for HILIC Method Development. https://www.phenomenex.com/ViewDocument?id=guidelines+for+hilic+method+development2019. (Accessed 04 June 2018).
[19] Column care and use instructions - YMC-Triart Diol HILIC. http://www.ymc.co.jp/data/download/Triart_Diol-HILIC_E.pdf19-9-2018. (Accessed 13 July 2018).
[20] Z. Hao, B. Xiao, N. Weng, Impact of column temperature and mobile phase components on selectivity of hydrophilic interaction chromatography (HILIC), J. Sep. Sci. 31 (2008) 1449–1464, http://dx.doi.org/10.1002/jssc.200700624.
[21] Y. Guo, S. Gaiki, Retention and selectivity of stationary phases for hydrophilic interaction chromatography, J. Chromatogr. A 1218 (2011) 5920–5938, http://dx.doi.org/10.1016/j.chroma.2011.06.052.
[22] D.V. McCalley, Understanding and manipulating the separation in hydrophilic interaction liquid chromatography, J. Chromatogr. A 1523 (2017) 49–71, http://dx.doi.org/10.1016/j.chroma.2017.06.026.
[23] Y.V. Kazakevich, R. LoBrutto, in: Y.V. Kazakevich, R. LoBrutto (Eds.), HPLC for Pharmaceutical Scientists, John Wiley & Sons, New York, 2007.
[24] X. Subirats, M. Rosés, E. Bosch, On the effect of organic solvent composition on the pH of buffered HPLC Mobile phases and the pK a of analytes—a review, Sep. Purif. Rev. 36 (2007) 231–255, http://dx.doi.org/10.1080/15422110701539129.
[25] R.-I. Chirita, C. West, A.-L. Finaru, C. Elfakir, Approach to hydrophilic interaction chromatography column selection: application to neurotransmitters analysis, J. Chromatogr. A 1217 (2010) 3091–3104, http://dx.doi.org/10.1016/j.chroma.2010.03.001.
[26] S. Espinosa, E. Bosch, M. Rosés, Retention of ionizable compounds on HPLC. 5. pH scales and the retention of acids and bases with acetonitrile–water Mobile phases, Anal. Chem. 72 (2000) 5193–5200, http://dx.doi.org/10.1021/ac000591b.
[27] I. Canals, K. Valko, E. Bosch, A.P. Hill, M. Rosés, Retention of ionizable compounds on HPLC. 8. Influence of mobile-phase pH change on the chromatographic retention of acids and bases during gradient elution, Anal. Chem. 73 (2001) 4937–4945.
[28] S. Espinosa, E. Bosch, M. Rosés, Retention of ionizable compounds in high-performance liquid chromatography: 14. Acid–base pK values in acetonitrile–water mobile phases, J. Chromatogr. A 964 (2002) 55–66, http://dx.doi.org/10.1016/S0021-9673(02)00558-7.
[29] M. Rosés, X. Subirats, E. Bosch, Retention models for ionizable compounds in reversed-phase liquid chromatography: effect of variation of mobile phase composition and temperature, J. Chromatogr. A 1216 (2009) 1756–1775, http://dx.doi.org/10.1016/j.chroma.2008.12.042.
[30] S.M.C. Buckenmaier, D.V. McCalley, M.R. Euerby, Rationalisation of unusual changes in efficiency and retention with temperature shown for bases in reversed-phase high-performance liquid chromatography at intermediate pH, J. Chromatogr. A 1060 (2004) 117–126, http://dx.doi.org/10.1016/j.chroma.2004.04.019.
[31] The Pesticide Manual - British Crop Production Council, https://www.bcpc.org (Accessed 19 September 2018).
[32] A.E. Karatapanis, Y.C. Fiamegos, C.D. Stalikas, A revisit to the retention mechanism of hydrophilic interaction liquid chromatography using model organic compounds, J. Chromatogr. A 1218 (2011) 2871–2879, http://dx.doi.org/10.1016/j.chroma.2011.02.069.
[33] P. Jandera, Stationary and mobile phases in hydrophilic interaction chromatography: a review, Anal. Chim. Acta 692 (2011) 1–25, http://dx.doi.org/10.1016/j.aca.2011.02.047.
[34] All positive/negative mode transitions - Ecxel Files on EPICS CD-ROM; Joint Analytical Systems GmbH, 2015.